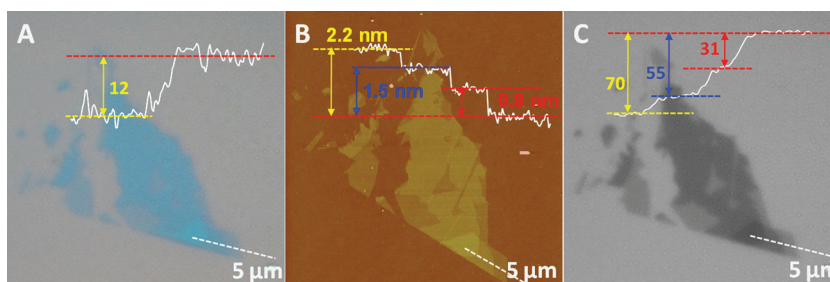


# Optical Identification of Single- and Few-Layer MoS<sub>2</sub> Sheets

Hai Li, Gang Lu, Zongyou Yin, Qiyuan He, Hong Li, Qing Zhang, and Hua Zhang\*

Two-dimensional (2D) layered nanomaterials have attracted increasing attention in recent years due to their unusual electronic and physical properties.<sup>[1–30]</sup> Among them, graphene, a single-layer 2D carbon material, has attracted enormous interest in both fundamental studies and potential applications.<sup>[1,2,4–6,30]</sup> Other 2D semiconducting dichalcogenides, such as MoS<sub>2</sub>, have also attracted significant research interest and show great potential applications.<sup>[1,3,7–24]</sup> Many methods have been reported to prepare the 2D layered nanomaterials, which include micromechanical cleavage,<sup>[1,6,18,21,22,25–29,31]</sup> chemical vapor deposition,<sup>[32]</sup> solution-based exfoliation,<sup>[12,16,20,23,24]</sup> and our recently developed simple but highly effective electrochemical lithiation process.<sup>[3]</sup> To date, micromechanical cleavage is still the easiest and fastest way to obtain highly crystalline, atomically layered sheets of 2D nanomaterials.<sup>[1,2,18,21,22,31,33,34]</sup>

The electronic properties of 2D layered nanomaterials are highly related to their thickness. Thus, the location and identification of the layer numbers of graphene and dichalcogenides is the first priority to enable the practical applications of these layered materials. Currently, many methods have been well established to identify the layer number of graphene, which include scanning probe microscopy (SPM),<sup>[1,4–6,30]</sup> scanning electron microscopy (SEM),<sup>[35]</sup> transmission electron microscopy (TEM),<sup>[36]</sup> Raman spectroscopy,<sup>[33,37–41]</sup> and optical microscopy.<sup>[34,35,42–50]</sup> Among them, Raman spectroscopy and optical microscopy can provide a rapid identification of single- and few-layer graphene sheets. However, it is still a challenge to identify the layer number of thin MoS<sub>2</sub>



**Figure 1.** Optical and AFM images of an MoS<sub>2</sub> flake consisting of 1L, 2L, and 3L sheets. A) Color optical image. Inset: Contrast profile of the dashed line showing the intensity difference between the MoS<sub>2</sub> flake and 300 nm SiO<sub>2</sub> substrate. B) AFM image. Inset: Height profile of the dashed line. C) Grayscale image of the R channel extracted from (A). Inset: Contrast profile of the dashed line showing the intensity difference between the MoS<sub>2</sub> flake and 300 nm SiO<sub>2</sub> substrate.

sheets rapidly and accurately using Raman spectroscopy, as the difference between double-layer and several-layer MoS<sub>2</sub> sheets is ambiguous and not obvious in Raman spectra.<sup>[10,22]</sup> Furthermore, until now there has been a paucity of reports on the identification of 2D layered dichalcogenide crystals by optical microscope,<sup>[18,51]</sup> especially the accurate identification of their layer number.

Herein, we present a simple, but rapid and accurate approach to identify the layer number of 2D layered MoS<sub>2</sub> sheets on a 300 nm SiO<sub>2</sub> substrate by using an optical imaging method combined with image analysis software (Image J). After the color optical image of MoS<sub>2</sub> sheets is split into the monochromatic red (R), green (G), and blue (B) channels using the Image J software, the high-contrast grayscale image of MoS<sub>2</sub> sheets can be found in the R channel. The intensity difference between the MoS<sub>2</sub> sheets (from single layer to triple layer) and 300 nm SiO<sub>2</sub> in the R channel increases with the layer number of MoS<sub>2</sub>, which can be used to identify the layer number of MoS<sub>2</sub> sheets. Atomic force microscopy (AFM) and Raman spectroscopy were also used to confirm the results obtained by the optical images.

In a typical experiment, we first used an optical microscope with a white-light source to locate the MoS<sub>2</sub> flake, obtained by the scotch tape-based mechanical exfoliation method,<sup>[22]</sup> and identify the layer number with the naked eye. AFM was then used to image the MoS<sub>2</sub> flake. **Figure 1A** shows the color optical image of a thin MoS<sub>2</sub> flake consisting of single- (1L), double- (2L), and triple-layer (3L) MoS<sub>2</sub> sheets (confirmed by AFM measurement in Figure 1B). As shown by the intensity profile (inset in Figure 1A), the value of the intensity difference between the 3L MoS<sub>2</sub> sheet

Dr. H. Li (Hai Li), G. Lu, Dr. Z. Y. Yin, Q. Y. He, Prof. H. Zhang  
School of Materials Science and Engineering  
Nanyang Technological University  
50 Nanyang Avenue, Singapore 639798, Singapore  
Homepage: <http://www.ntu.edu.sg/home/hzhang/>  
E-mail: [h Zhang@ntu.edu.sg](mailto:h Zhang@ntu.edu.sg); [h Zhang166@yahoo.com](mailto:h Zhang166@yahoo.com)  
Dr. H. Li (Hong Li), Prof. Q. Zhang  
Microelectronics Center  
School of Electrical and Electronics Engineering  
Nanyang Technological University  
50 Nanyang Avenue, Singapore 639798, Singapore



DOI: 10.1002/sml.201101958

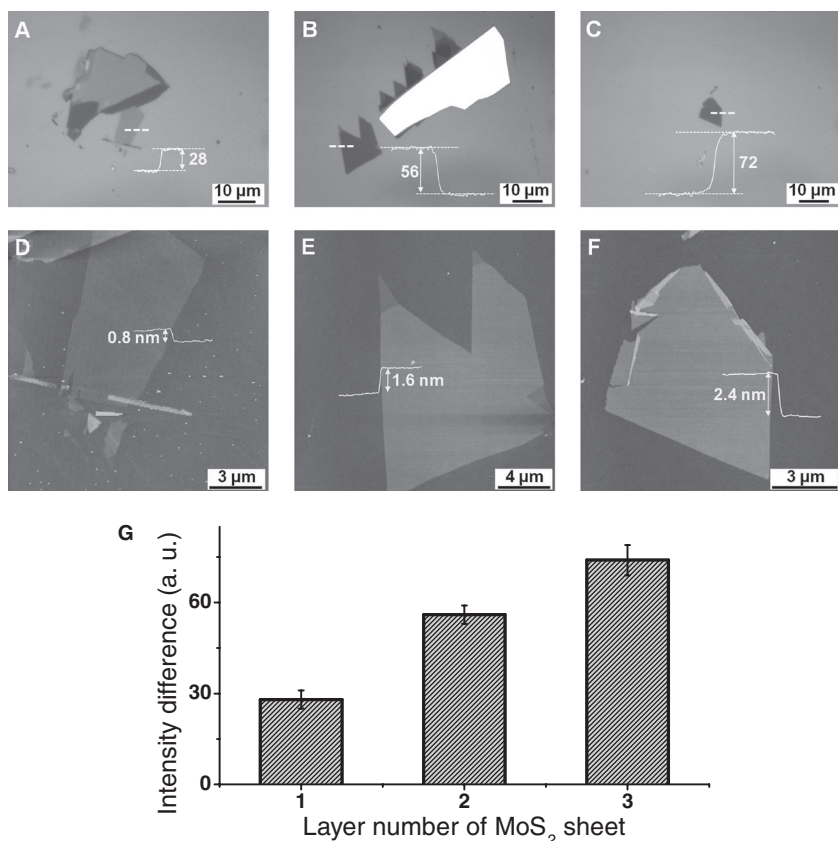


**Figure 2.** Grayscale images of the R channel of A) 1L, B) 2L, and C) 3L MoS<sub>2</sub> sheets and D–F) the corresponding AFM images. The inset in each image is the corresponding contrast profile or height profile. G) Statistical data of the intensity difference between MoS<sub>2</sub> sheets (1L, 2L, and 3L) and the 300 nm SiO<sub>2</sub> substrate.

(further confirmed by AFM measurement in Figure 1B) and the 300 nm SiO<sub>2</sub> substrate is 12 and the boundaries among the 1L, 2L, and 3L MoS<sub>2</sub> sheets are ambiguous. Therefore, it is difficult to identify the different atomic planes of the MoS<sub>2</sub> flake from the color optical microscopy image.

It has been reported that the layer numbers of single- and few-layer graphene sheets can be determined by analyzing their intensity difference in the grayscale image converted from the color optical image,<sup>[50]</sup> but this method does not work on the 1L to 3L MoS<sub>2</sub> sheets (Figure S1A,B in the Supporting Information). However, we found that after the color optical image of MoS<sub>2</sub> flake (Figure 1A) was split into the grayscale images of R, G, and B channels using the Image J software, the grayscale image of the R channel showed a high-contrast image of the MoS<sub>2</sub> flake (Figure 1C), while that of G or B channels showed low-contrast images (Figure S1C,D in the Supporting Information). As shown in Figure 1C, the 1L, 2L, and 3L MoS<sub>2</sub> sheets (confirmed by AFM in Figure 1B) can be clearly distinguished and the intensity profile (inset in Figure 1C) shows three clearly observed steps, which correspond to the different layers of MoS<sub>2</sub> sheets.

AFM was further used to image the same MoS<sub>2</sub> flake shown in Figure 1A and C. The height profile clearly showed that the thickness of the three steps is 0.8, 1.5, and 2.2 nm (Figure 1B), which is consistent with the height of 1L, 2L, and

3L MoS<sub>2</sub> sheets, respectively.<sup>[22]</sup> These data confirm that the three steps in the intensity profile shown in Figure 1C correspond to the 1L, 2L, and 3L MoS<sub>2</sub> sheets. The values of the intensity difference between the MoS<sub>2</sub> sheet and 300 nm SiO<sub>2</sub> substrate (inset in Figure 1C) are 31 for 1L MoS<sub>2</sub>, 55 for 2L MoS<sub>2</sub>, and 70 for 3L MoS<sub>2</sub>.

To give quantitative and statistical characterization of the layer numbers of MoS<sub>2</sub> sheets, a large number of MoS<sub>2</sub> flakes (total 77 flakes) with layer numbers ranging from 1L to 3L, prepared by the mechanical cleavage technique,<sup>[22]</sup> were measured by optical microscopy and AFM. **Figure 2A–C** show the typical optical images of individual 1L (Figure 2A), 2L (Figure 2B), and 3L (Figure 2C) MoS<sub>2</sub> sheets. The value of the intensity difference between these MoS<sub>2</sub> sheets and the 300 nm SiO<sub>2</sub> substrate is 28 for 1L MoS<sub>2</sub>, 56 for 2L MoS<sub>2</sub>, and 72 for 3L MoS<sub>2</sub> (insets in Figure 2A, B, and C, respectively). Figure 2D–F shows the corresponding AFM images, which further confirmed the layer numbers of the corresponding MoS<sub>2</sub> sheets (Figure 2A–C), that is, 0.8 nm for 1L, 1.6 nm for 2L, and 2.4 nm for 3L MoS<sub>2</sub>. The statistical data of the value of intensity difference between the MoS<sub>2</sub> sheet and substrate with respect to different

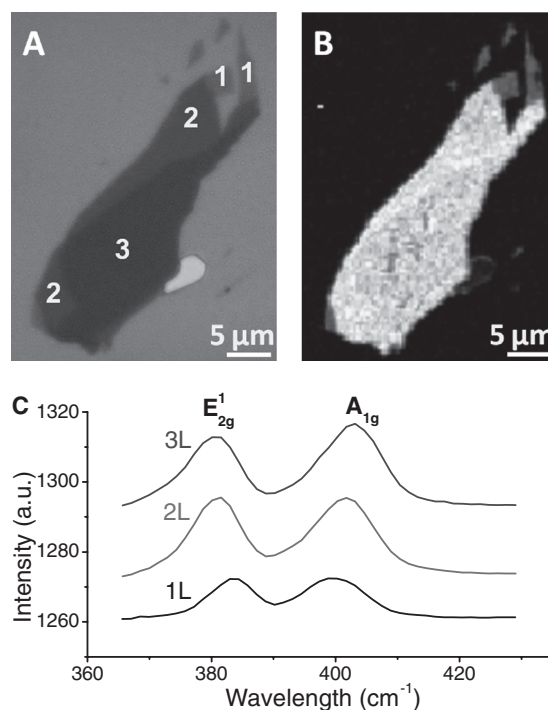


**Figure 3.** A) Grayscale image of the R channel and B) Raman mapping of an MoS<sub>2</sub> flake. Three regions with different contrast marked by 1, 2, and 3 correspond to 1L, 2L, and 3L MoS<sub>2</sub> sheets, respectively. C) Raman spectra of 1L, 2L, and 3L MoS<sub>2</sub> sheets.

layer numbers are plotted in Figure 2G, which shows that the values of intensity difference for 1L, 2L, and 3L MoS<sub>2</sub> sheets are  $28 \pm 3$ ,  $56 \pm 3$ , and  $74 \pm 5$ , respectively. Therefore, our method provides a quantitative fingerprint to distinguish the layer number (1L to 3L) of MoS<sub>2</sub> sheets on the 300 nm SiO<sub>2</sub> substrate.

Moreover, Raman spectroscopy was used to confirm the successful identification of the layer number of MoS<sub>2</sub> by using the aforementioned method. **Figure 3A** shows the grayscale image of the R channel of an MoS<sub>2</sub> flake. It is clearly observed that the MoS<sub>2</sub> flake has three regions with different contrast marked by 1, 2, and 3, which corresponded to 1L, 2L, and 3L MoS<sub>2</sub> sheets, respectively, confirmed by our aforementioned method. The Raman spectra of the marked regions (Figure 3C) further confirmed the layer numbers of the MoS<sub>2</sub> flakes. The 1L MoS<sub>2</sub> sheet exhibits strong bands at 384 and 400 cm<sup>-1</sup>, which are associated with the in-plane vibration ( $E_{2g}^1$ ) and out-of-plane vibration ( $A_{1g}$ ) modes, respectively. As the layer number increases from 1L to 3L (Figure 3C), a red shift of the  $E_{2g}^1$  band and a blue shift of the  $A_{1g}$  band were observed, which is consistent with previous reports.<sup>[10,22]</sup> However, in the Raman mapping (Figure 3B), although 1L and 2L of MoS<sub>2</sub> sheets can be easily identified, the contrast between 2L and 3L MoS<sub>2</sub> sheets is quite low.

To study the electrical properties of different layered MoS<sub>2</sub> sheets, field-effect transistors (FETs) were fabricated. The recorded  $I_{ds}$ - $V_g$  characteristic curve (**Figure 4A**) is typical of a 1L MoS<sub>2</sub> FET with an n-type channel, which is in agreement with previous reports.<sup>[10,22]</sup> Similarly, the 2L and 3L MoS<sub>2</sub> FETs also showed the n-type doping characteristic (Figure 4B and C). The current On/Off ratio of the fabricated 1L, 2L, and 3L MoS<sub>2</sub> devices is above  $10^3$  ( $V_g$  ranging from -20 to +20 V, Figure 4A–C). Figure 4D–F shows the  $I_{ds}$ - $V_{ds}$  curves of 1L to 3L MoS<sub>2</sub> FETs at  $V_g$  from -20 to +20 V.

In summary, a simple approach is developed to rapidly and accurately identify 1L to 3L MoS<sub>2</sub> sheets on a 300 nm SiO<sub>2</sub> substrate by using an optical microscopy imaging method combined with the Image J software. The grayscale image of the R channel, which is extracted from the color optical image, shows a high-contrast image of the MoS<sub>2</sub> sheet with thickness ranging from 1L to 3L. The value of the intensity difference between MoS<sub>2</sub> sheets (1L to 3L) and the 300 nm SiO<sub>2</sub> substrate in the grayscale image of the R channel is successfully used to identify the layer number of MoS<sub>2</sub> sheets quantitatively. AFM and Raman spectroscopy are also used to confirm the data obtained by the aforementioned method. Our technique provides an effective and quantitative fingerprint to quickly and accurately distinguish the 1L to 3L MoS<sub>2</sub>

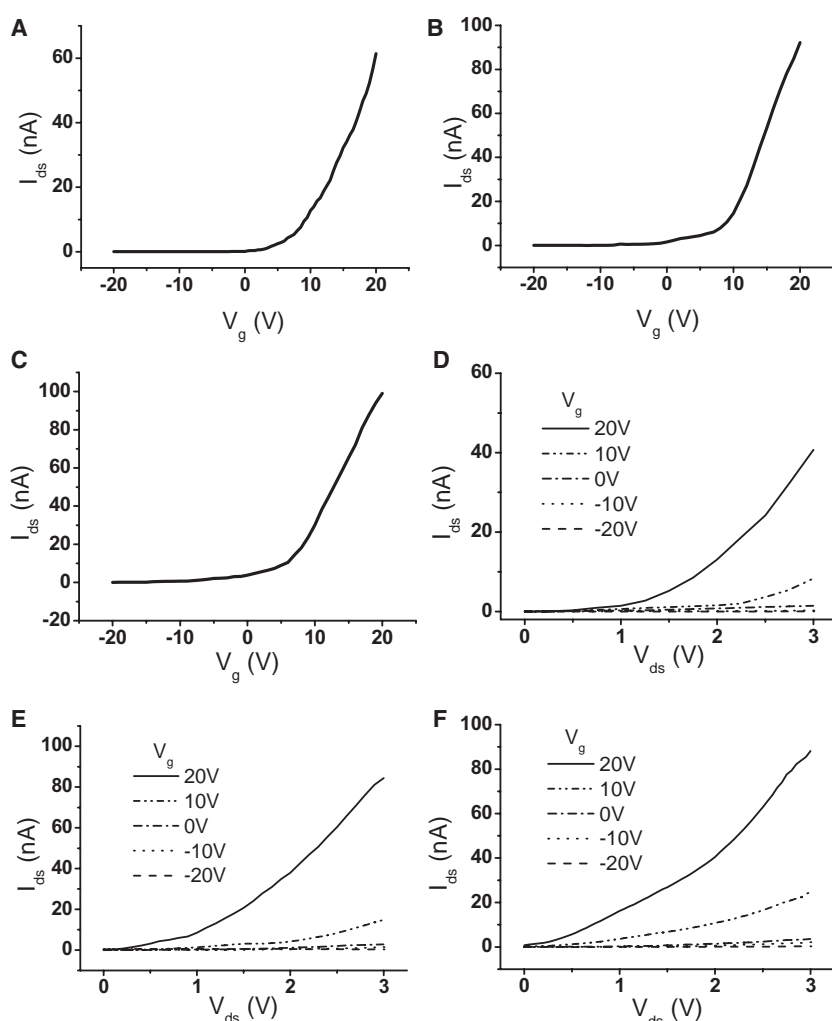


**Figure 4.** A–C) Plots of  $I_{ds}$  versus  $V_g$  of A) 1L, B) 2L, and C) 3L MoS<sub>2</sub>-based FETs at  $V_{ds} = 3$  V. D–F)  $I_{ds}$ - $V_{ds}$  curves of D) 1L, E) 2L, and F) 3L MoS<sub>2</sub>-based FETs at different  $V_g$  from -20 to +20 V.

sheets on the 300 nm SiO<sub>2</sub> substrate, which is useful in device fabrication using different layered MoS<sub>2</sub> sheets.

## Experimental Section

**Mechanical Exfoliation of MoS<sub>2</sub>:** Single- and few-layer MoS<sub>2</sub> sheets were isolated from a bulk MoS<sub>2</sub> sample (429MM-AB, molybdenum disulfide, single crystals from Canada, SPI Supplies) and then deposited onto freshly cleaned Si substrates covered by a 300-nm-thick SiO<sub>2</sub> layer by using the scotch tape-based mechanical exfoliation method,<sup>[22]</sup> which is widely employed for the preparation of single-layer graphene sheets.

**Optical Microscopy Imaging and Data Analysis Using Image J Software:** First, an optical microscope (Eclipse LV100D with a 100 $\times$ , 0.9 numerical aperture (NA) objective, Nikon) equipped with a color camera (Nikon DS-Fi1) was used to locate and identify the 1L to 3L MoS<sub>2</sub> sheets with the naked eye. The color optical images of 1L to 3L MoS<sub>2</sub> sheets were captured by using the NIS Elements software (NIS-Elements F Package Ver. 3.00, Nikon). To calibrate and obtain the color images of MoS<sub>2</sub> sheets with a similar contrast, the “autowhite” command was applied before the images were captured.



The color optical images of 1L to 3L MoS<sub>2</sub> sheets were opened by the ImageJ software (version 1.45o, National Institutes of Health, USA), and the grayscale image of the R channel was extracted by using the "Split Channels" command from "Image>Color>Split Channels" in the menu. In the grayscale image of the R channel, we dragged the left button of the mouse to draw a line across the atomically thin MoS<sub>2</sub> sheet and then pressed "Ctrl+K" to obtain the line profile of intensity difference. In the plot of the line profile, we clicked "List" to show the intensity values of the MoS<sub>2</sub> sheet and SiO<sub>2</sub> substrate.

**AFM Images and Raman Spectroscopy:** AFM (Dimension 3100 with Nanoscope IIIa controller, Veeco, CA, USA) was used to image the MoS<sub>2</sub> sheets in tapping mode in air and confirm the layer number by measuring the thickness of the MoS<sub>2</sub> sheets. Analysis of 1L to 3L MoS<sub>2</sub> sheets by Raman spectroscopy was carried out on a WITec CRM200 confocal Raman microscopy system with the excitation line of 488 nm and an air-cooled charge-coupled device (CCD) as the detector (WITec Instruments Corp., Germany). The Raman band of a Si wafer at 520 cm<sup>-1</sup> was used as a reference to calibrate the spectrometer.

**Fabrication and Characterization of MoS<sub>2</sub> FETs:** The source and drain electrodes of MoS<sub>2</sub> FET devices were fabricated by the traditional photolithography. The channel length for all FET devices was kept at ≈3 μm. The 5 nm Ti/50 nm Au source and drain electrodes were deposited by using an electron-beam evaporator. After removal of the photoresist with acetone and subsequent thermal annealing at 200 °C for 2 h in the mixture of Ar:H<sub>2</sub> (v/v=9:1),<sup>[22a]</sup> the electrical properties of 1L to 3L MoS<sub>2</sub> FETs were tested by the Keithley 4200 semiconductor characterization system in air at room temperature.

## Supporting Information

Supporting Information is available from the Wiley Online Library or from the author.

## Acknowledgements

This work was supported by AcRF Tier 2 (ARC 10/10, No. MOE2010-T2-1-060) from MOE, the Singapore National Research Foundation under CREATE programme: Nanomaterials for Energy and Water Management, and the New Initiative Fund FY 2010 (M58120031) from NTU in Singapore.

- [1] K. S. Novoselov, D. Jiang, F. Schedin, T. J. Booth, V. V. Khotkevich, S. V. Morozov, A. K. Geim, *Proc. Natl. Acad. Sci. USA* **2005**, *102*, 10451.
- [2] A. K. Geim, K. S. Novoselov, *Nat. Mater.* **2007**, *6*, 183.
- [3] Z. Zeng, Z. Yin, X. Huang, H. Li, Q. He, G. Lu, F. Boey, H. Zhang, *Angew. Chem. Int. Ed.* **2011**, *50*, 11093.
- [4] Q. Y. He, H. G. Sudibya, Z. Y. Yin, S. X. Wu, H. Li, F. Boey, W. Huang, P. Chen, H. Zhang, *ACS Nano* **2010**, *4*, 3201.
- [5] X. Huang, Z. Y. Yin, S. X. Wu, X. Y. Qi, Q. Y. He, Q. C. Zhang, Q. Y. Yan, F. Boey, H. Zhang, *Small* **2011**, *7*, 1876.

- [6] K. S. Novoselov, A. K. Geim, S. V. Morozov, D. Jiang, Y. Zhang, S. V. Dubonos, I. V. Grigorieva, A. A. Firsov, *Science* **2004**, *306*, 666.
- [7] A. Ayari, E. Cobas, O. Ogundadegbe, M. S. Fuhrer, *J. Appl. Phys.* **2007**, *101*, 014507.
- [8] S. S. Hong, W. Kundhikanjana, J. J. Cha, K. J. Lai, D. S. Kong, S. Meister, M. A. Kelly, Z. X. Shen, Y. Cui, *Nano Lett.* **2010**, *10*, 3118.
- [9] C. Lee, Q. Y. Li, W. Kalb, X. Z. Liu, H. Berger, R. W. Carpick, J. Hone, *Science* **2010**, *328*, 76.
- [10] C. Lee, H. Yan, L. E. Brus, T. F. Heinz, J. Hone, S. Ryu, *ACS Nano* **2010**, *4*, 2695.
- [11] K. F. Mak, C. Lee, J. Hone, J. Shan, T. F. Heinz, *Phys. Rev. Lett.* **2010**, *105*, 136805.
- [12] H. S. S. R. Matte, A. Gomathi, A. K. Manna, D. J. Late, R. Datta, S. K. Pati, C. N. R. Rao, *Angew. Chem. Int. Ed.* **2010**, *49*, 4059.
- [13] A. Splendiani, L. Sun, Y. B. Zhang, T. S. Li, J. Kim, C. Y. Chim, G. Galli, F. Wang, *Nano Lett.* **2010**, *10*, 1271.
- [14] D. Teweldebrhan, V. Goyal, A. A. Balandin, *Nano Lett.* **2010**, *10*, 1209.
- [15] Z. Y. Wang, H. Li, Z. Liu, Z. J. Shi, J. Lu, K. Suenaga, S. K. Joung, T. Okazaki, Z. N. Gu, J. Zhou, Z. X. Gao, G. P. Li, S. Sanvito, E. G. Wang, S. Iijima, *J. Am. Chem. Soc.* **2010**, *132*, 13840.
- [16] J. Xiao, D. W. Choi, L. Cosimbescu, P. Koech, J. Liu, J. P. Lemmon, *Chem. Mater.* **2010**, *22*, 4522.
- [17] C. Ataca, H. Sahin, E. Akturk, S. Ciraci, *J. Phys. Chem. C* **2011**, *115*, 3934.
- [18] M. M. Benameur, B. Radisavljevic, J. S. Heron, S. Sahoo, H. Berger, A. Kis, *Nanotechnology* **2011**, *22*, 125706.
- [19] S. Cho, N. P. Butch, J. Paglione, M. S. Fuhrer, *Nano Lett.* **2011**, *11*, 1925.
- [20] J. N. Coleman, M. Lotya, A. O'Neill, S. D. Bergin, P. J. King, U. Khan, K. Young, A. Gaucher, S. De, R. J. Smith, I. V. Shvets, S. K. Arora, G. Stanton, H. Y. Kim, K. Lee, G. T. Kim, G. S. Duesberg, T. Hallam, J. J. Boland, J. J. Wang, J. F. Donegan, J. C. Grunlan, G. Moriarty, A. Shmeliov, R. J. Nicholls, J. M. Perkins, E. M. Grievson, K. Theuvsen, D. W. McComb, P. D. Nellist, V. Nicolosi, *Science* **2011**, *331*, 568.
- [21] B. Radisavljevic, A. Radenovic, J. Brivio, V. Giacometti, A. Kis, *Nat. Nanotechnol.* **2011**, *6*, 147.
- [22] a) Z. Y. Yin, H. Li, H. Li, L. Jiang, Y. M. Shi, Y. H. Sun, G. Lu, Q. Zhang, X. D. Chen, H. Zhang, *ACS Nano* **2012**, DOI: 10.1021/nn2024557; b) H. Li, Z. Y. Yin, Q. Y. He, H. Li, X. Huang, G. Lu, D. W. H. Fam, A. I. Y. Tok, Q. Zhang, H. Zhang, *Small* **2012**, *8*, 63.
- [23] R. J. Smith, P. J. King, M. Lotya, C. Wirtz, U. Khan, S. De, A. O'Neill, G. S. Duesberg, J. C. Grunlan, G. Moriarty, J. Chen, J. Wang, A. I. Minett, V. Nicolosi, J. N. Coleman, *Adv. Mater.* **2011**, *23*, 3944.
- [24] K.-G. Zhou, N.-N. Mao, H.-X. Wang, Y. Peng, H.-L. Zhang, *Angew. Chem. Int. Ed.* **2011**, *50*, 10839.
- [25] V. Goyal, D. Teweldebrhan, A. A. Balandin, *Appl. Phys. Lett.* **2010**, *97*, 133117.
- [26] K. M. F. Shahil, M. Z. Hossain, D. Teweldebrhan, A. A. Balandin, *Appl. Phys. Lett.* **2010**, *96*, 153103.
- [27] D. Teweldebrhan, V. Goyal, M. Rahman, A. A. Balandin, *Appl. Phys. Lett.* **2010**, *96*, 053107.
- [28] M. Z. Hossain, S. L. Rumyantsev, K. M. F. Shahil, D. Teweldebrhan, M. Shur, A. A. Balandin, *ACS Nano* **2011**, *5*, 2657.
- [29] M. Z. Hossain, S. L. Rumyantsev, D. Teweldebrhan, K. M. F. Shahil, M. Shur, A. A. Balandin, *Phys. Status Solidi A* **2011**, *208*, 144.
- [30] X. Huang, X. Qi, F. Boey, H. Zhang, *Chem. Soc. Rev.* **2012**, DOI: 10.1039/C1CS15078B.
- [31] A. Reina, H. Son, L. Jiao, B. Fan, M. S. Dresselhaus, Z. Liu, J. Kong, *J. Phys. Chem. C* **2008**, *112*, 17741.
- [32] X. S. Li, W. W. Cai, J. H. An, S. Kim, J. Nah, D. X. Yang, R. Piner, A. Velamakanni, I. Jung, E. Tutuc, S. K. Banerjee, L. Colombo, R. S. Ruoff, *Science* **2009**, *324*, 1312.

- [33] Y. F. Hao, Y. Y. Wang, L. Wang, Z. H. Ni, Z. Q. Wang, R. Wang, C. K. Koo, Z. X. Shen, J. T. L. Thong, *Small* **2010**, *6*, 195.
- [34] Z. H. Ni, H. M. Wang, J. Kasim, H. M. Fan, T. Yu, Y. H. Wu, Y. P. Feng, Z. X. Shen, *Nano Lett.* **2007**, *7*, 2758.
- [35] S. Roddaro, P. Pingue, V. Piazza, V. Pellegrini, F. Beltram, *Nano Lett.* **2007**, *7*, 2707.
- [36] J. C. Meyer, A. K. Geim, M. I. Katsnelson, K. S. Novoselov, T. J. Booth, S. Roth, *Nature* **2007**, *446*, 60.
- [37] A. Gupta, G. Chen, P. Joshi, S. Tadigadapa, P. C. Eklund, *Nano Lett.* **2006**, *6*, 2667.
- [38] A. C. Ferrari, J. C. Meyer, V. Scardaci, C. Casiraghi, M. Lazzeri, F. Mauri, S. Piscanec, D. Jiang, K. S. Novoselov, S. Roth, A. K. Geim, *Phys. Rev. Lett.* **2006**, *97*, 187401.
- [39] D. Graf, F. Molitor, K. Ensslin, C. Stampfer, A. Jungen, C. Hierold, L. Wirtz, *Nano Lett.* **2007**, *7*, 238.
- [40] J. M. Caridad, F. Rossella, V. Bellani, M. S. Grandi, E. Diez, *J. Raman Spectrosc.* **2011**, *42*, 286.
- [41] Y. K. Koh, M. H. Bae, D. G. Cahill, E. Pop, *ACS Nano* **2011**, *5*, 269.
- [42] P. Blake, E. W. Hill, A. H. C. Neto, K. S. Novoselov, D. Jiang, R. Yang, T. J. Booth, A. K. Geim, *Appl. Phys. Lett.* **2007**, *91*, 063124.
- [43] I. Jung, M. Pelton, R. Piner, D. A. Dikin, S. Stankovich, S. Watcharotone, M. Hausner, R. S. Ruoff, *Nano Lett.* **2007**, *7*, 3569.
- [44] L. B. Gao, W. C. Ren, F. Li, H. M. Cheng, *ACS Nano* **2008**, *2*, 1625.
- [45] Y. F. Chen, D. Liu, Z. G. Wang, P. J. Li, X. Hao, K. Cheng, Y. Fu, L. X. Huang, X. Z. Liu, W. L. Zhang, Y. R. Li, *J. Phys. Chem. C* **2011**, *115*, 6690.
- [46] M. Bruna, S. Borini, *Appl. Phys. Lett.* **2009**, *94*, 031901.
- [47] P. E. Gaskell, H. S. Skulason, C. Rodenchuk, T. Szkopek, *Appl. Phys. Lett.* **2009**, *94*, 143101.
- [48] M. Dorn, P. Lange, A. Chekushin, N. Severin, J. P. Rabe, *J. Appl. Phys.* **2010**, *108*, 106101.
- [49] Z. Fei, Y. Shi, L. Pu, F. Gao, Y. Liu, L. Sheng, B. G. Wang, R. Zhang, Y. D. Zheng, *Phys. Rev. B* **2008**, *78*, 201402.
- [50] K. Nagashio, T. Nishimura, K. Kita, A. Toriumi, *Appl. Phys. Express* **2009**, *2*, 025003.
- [51] A. Castellanos-Gomez, N. Agrait, G. Rubio-Bollinger, *Appl. Phys. Lett.* **2010**, *96*, 213116.

Received: September 20, 2011  
Published online: January 5, 2012